



Cite this: *Metallomics*, 2015, 7, 691

## *Rhizobium leguminosarum* HupE is a highly-specific diffusion facilitator for nickel uptake†

Marta Albareda,<sup>‡a</sup> Agnès Rodrigue,<sup>b</sup> Belén Brito,<sup>a</sup> Tomás Ruiz-Argüeso,<sup>a</sup> Juan Imperial,<sup>a,c</sup> Marie-Andrée Mandrand-Berthelot<sup>\*b</sup> and Jose Palacios<sup>\*a</sup>

Bacteria require nickel transporters for the synthesis of Ni-containing metalloenzymes in natural, low nickel habitats. In this work we carry out functional and topological characterization of *Rhizobium leguminosarum* HupE, a nickel permease required for the provision of this element for [NiFe] hydrogenase synthesis. Expression studies in the *Escherichia coli* *nikABCDE* mutant strain HYD723 revealed that HupE is a medium-affinity permease (apparent  $K_m$   $227 \pm 21$  nM;  $V_{max}$   $49 \pm 21$  pmol  $Ni^{2+}$   $min^{-1}$   $mg^{-1}$  bacterial dry weight) that functions as an energy-independent diffusion facilitator for the uptake of Ni(II) ions. This  $Ni^{2+}$  transport is not inhibited by similar cations such as  $Mn^{2+}$ ,  $Zn^{2+}$ , or  $Co^{2+}$ , but is blocked by  $Cu^{2+}$ . Analysis of site-directed HupE mutants allowed the identification of several residues (H36, D42, H43, F69, E90, H130, and E133) that are essential for HupE-mediated Ni uptake in *E. coli* cells. By using translational fusions to reporter genes we demonstrated the presence of five transmembrane domains with a periplasmic N-terminal domain and a C-terminal domain buried in the lipid bilayer. The periplasmic N-terminal domain contributes to stability and functionality of the protein.

Received 15th November 2014,  
Accepted 27th January 2015

DOI: 10.1039/c4mt00298a

[www.rsc.org/metallomics](http://www.rsc.org/metallomics)

## Introduction

Nickel is a transition metal required for many biological processes as a component of cofactors in at least nine enzymes: hydrogenase, urease, carbon monoxide dehydrogenase, acetyl-CoA synthase, superoxide dismutase, methyl coenzyme-M reductase, acireductone dioxygenase, glyoxalase and lactate racemase.<sup>1</sup> Apart from urease, these nickel enzymes reside exclusively in micro-organisms. Most natural environments contain only traces of soluble Ni, and bacteria have developed high-affinity uptake systems required for the synthesis of these metalloenzymes.<sup>2,3</sup> Nickel transport systems of two main types have been described in bacteria: ATP-binding cassette (ABC)-type transporters, and single permeases. ABC-type nickel transport systems comprise two families: NikABCDE and NikMNQO-CbiMNQO.<sup>4,5</sup> The NikABCDE system

includes a periplasmic, high-affinity nickel binding protein (Nika) responsible for capturing nickel ions in the periplasm thus delivering them to the NikBC membrane pore.<sup>6</sup> Such a periplasmic protein is absent from the Nik-CbiMNQO systems,<sup>5</sup> suggesting a different mode of action for both families of ABC-type transporters.

Nickel permeases are single component transporters with multiple transmembrane domains. Three groups of permeases have been described: NiCoTs, UreH, and HupE/UreJ. Members of the NiCoT family are grouped into three classes depending on whether they are highly specific for nickel (Class I), prefer cobalt over nickel (Class II) or prefer nickel over cobalt (Class III).<sup>7</sup> The best-studied proteins within this family are the Class I nickel transporters *Cupriavidus necator* HoxN<sup>8</sup> and *Helicobacter pylori* NixA.<sup>9</sup> Both proteins are high-affinity nickel transporters with an apparent  $K_m$  in the low nanomolar range.<sup>9,10</sup> These two proteins share a topology with eight transmembrane domains,<sup>11,12</sup> and two conserved histidine-rich motifs critical for metal uptake (GX<sub>2</sub>HX<sub>4</sub>DH and GX<sub>2</sub>FX<sub>2</sub>GH).<sup>11,13</sup> The UreH group includes Ni-specific permeases whose corresponding genes are associated with gene clusters for urease or Ni-superoxide dismutase in the genome of *Bacillus* and also in several proteobacteria and cyanobacteria.<sup>5,14</sup> Finally, members of the HupE/UreJ family are widespread among bacteria, and are usually encoded within hydrogenase or urease gene clusters.<sup>5</sup> In some cyanobacteria the *hupE*-like genes are preceded by B<sub>12</sub> riboswitches, thus suggesting a preference for cobalt ions.<sup>15</sup> *Rhizobium leguminosarum* HupE was the first member of the HupE/UreJ family specifically

<sup>a</sup> Departamento de Biotecnología, Escuela Técnica Superior de Ingenieros Agrónomos and Centro de Biotecnología y Genómica de Plantas (C.B.G.P.), Universidad Politécnica de Madrid, Campus de Montegancedo, Carretera M40-km 38, 28223 Pozuelo de Alarcón, Madrid, Spain. E-mail: jose.palacios@upm.es

<sup>b</sup> Microbiologie, Adaptation et Pathogénie, UMR5240 CNRS INSA Lyon Université Lyon 1, Bat. Lwoff, 10 rue Dubois, F-69622 Villeurbanne Cedex, France. E-mail: marie-andree.mandrand@insa-lyon.fr

<sup>c</sup> Consejo Superior de Investigaciones Científicas (CSIC), Centro de Biotecnología and Genómica de Plantas (C.B.G.P.), Universidad Politécnica de Madrid (U.P.M.), Spain

† Electronic supplementary information (ESI) available. See DOI: 10.1039/c4mt00298a

‡ Present address: Division of Molecular Microbiology, College of Life Sciences, University of Dundee, Dundee DD1 5EH, Scotland, UK.

described as a nickel transporter required for hydrogenase synthesis.<sup>16</sup> Algorithm-based topology analysis of HupE protein predicted the existence of six transmembrane domains (TMD). Sequence alignment of multiple *hupE/uref* genes allowed the identification of two conserved histidine-rich motifs (HX<sub>5</sub>DH in TMD I and FHGX[AV]HGXE in TMD IV), and site-directed mutagenesis has shown that histidine residues contained in these motifs are essential for HupE functionality.<sup>16</sup> In that work it was also shown that the *R. leguminosarum* UPM791 genome contains genes for two HupE-like proteins (HupE and HupE2). HupE is encoded within the hydrogenase gene cluster in the symbiotic plasmid, whereas HupE2 is encoded in a different plasmid.

An important aspect of nickel transport is the potential relevance of the formation of complexes with organic ligands, which might be required for transport. In the case of the Nik system, crystallographic and spectroscopic data indicate that Ni(II) is bound to NikA as a complex with a small organic molecule, modeled as a butane tricarboxylate,<sup>17</sup> although the biological relevance of this complex could not be demonstrated. A recent study has shown that NikA binds a (L-His)<sub>2</sub>-Ni complex, and that Ni(II) and L-His are likely co-transported through the *E. coli* NikABCDE system.<sup>18</sup> The presence of a similar complex has been demonstrated for the periplasmic binding protein CeuE in *H. pylori*.<sup>19</sup> It has been hypothesized that the presence of nickel complexes could occur in other systems. *H. pylori* nickel uptake is partially dependent on a TonB-dependent outer membrane receptor with homology to known iron-complex transporters, thus suggesting the potential participation of a nickelophore in the transport process.<sup>20</sup> It has also been found that nickel is complexed with organic acids malate and citrate in the cytoplasm of root legume nodules,<sup>21</sup> the natural habitat from which the endosymbiotic bacterium *R. leguminosarum* takes up nickel for synthesis of NiFe hydrogenase. However, the relevance of such ligands for nickel uptake was not demonstrated at that time.

High-affinity nickel transport systems might require a source of energy to accumulate Ni(II) intracellularly against a concentration gradient. ABC-transporters couple the binding and hydrolysis of ATP to the translocation of the metal across the cytoplasmic membrane.<sup>22</sup> However, no clear picture on the energy requirements of nickel permeases is available. On the basis of the effect of metabolic inhibitors and ionophores it has been proposed that the proton motive force is likely to be involved in Ni transport in *Clostridium thermoaceticum*,<sup>23</sup> and that Ni transport in *Methanobacterium bryantii* is coupled to proton movement.<sup>24</sup> Accumulation of nickel ions in the cyanobacterium *Anabaena cylindrica* is dependent on the electrochemical potential gradient that is collapsed by uncouplers.<sup>25</sup> However, these observations should be considered with caution since first, these experiments were not performed with the isolated permease expressed from the corresponding cloned gene and thus reflected the bulk of cellular Ni transport; and second, some of the above-cited bacteria might possess more than one Ni transporter, as for the cyanobacterium *Anabaena variabilis* which contains the two Ni transporters HupE and NikMNQO.<sup>5</sup> In accord with this point,

a previous study supported the dependence of Ni transport in *A. eutrophus* on the availability of an energy source.<sup>26</sup> These data were further contradicted by subsequent analysis showing that the HoxN-mediated Ni uptake was unaffected by the addition of a mixture of the two selective ionophores valinomycin (collapsing the membrane potential) and nigericin (collapsing the pH gradient).<sup>27</sup> Along the same lines, nickel uptake in *Bradyrhizobium japonicum* strain SR470 was not inhibited by the metabolic inhibitor azide and only marginally inhibited by carbonyl cyanide *m*-chlorophenylhydrazone (CCCP) and *N,N'*-dicyclohexylcarbodiimide (DCCD), which suggested that the transport process was likely independent of energy.<sup>28</sup>

In this work we carry out functional and topological characterization of *R. leguminosarum* HupE. The results obtained indicate that HupE is a medium-affinity permease with multiple transmembrane domains that functions as an energy-independent diffusion facilitator for the specific uptake of Ni(II) ions.

## Results

### 1. Kinetic analysis of nickel transport through HupE

In a previous report we demonstrated that *R. leguminosarum* HupE mediates Ni(II) transport when expressed in *E. coli* cells.<sup>16</sup> Heterologous expression in this background allowed us to overcome the problem of excessive unspecific Ni binding to *Rhizobium* cells.<sup>16</sup> Here, to determine the kinetic parameters of nickel transport, we examined in more detail the Ni(II) uptake rates in HupE-expressing *E. coli* cells exposed to different concentrations of this element (Fig. 1). We concluded that HupE-dependent Ni(II) uptake is a concentration-dependent and saturable process that fits a Michaelis-Menten equation with an apparent  $K_m$  value of  $227 \pm 21$  nM and a  $V_{max}$  value of  $49 \pm 21$  pmol min<sup>-1</sup> mg<sup>-1</sup> bacterial dry weight (BDW).

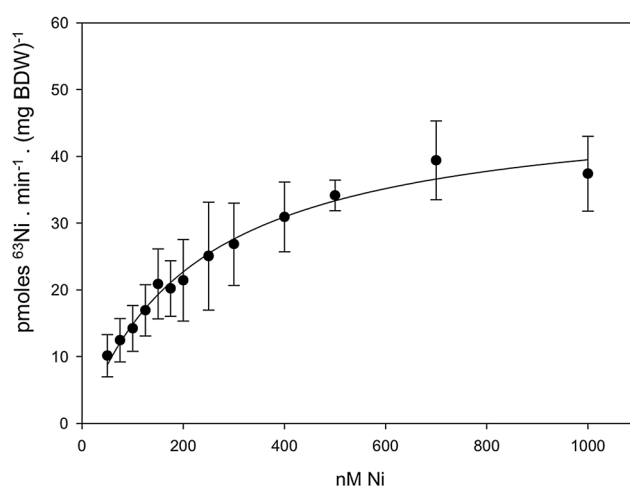


Fig. 1 Kinetic analysis of HupE-mediated Ni(II) transport. HupE-expressing *E. coli* cells were incubated for 45 s, 90 s and 135 s in the presence of different amounts of <sup>63</sup>Ni(II), and the amount of radioactivity incorporated was measured. Values are the average of at least three independent experiments  $\pm$  S.D.

Ni uptake assays were carried out with cells in a buffer containing free Ni(II) ions. Under natural conditions for HupE expression in *R. leguminosarum* (i.e., in bacteroids within legume nodules) nickel available to the bacteroids is usually not present as a free ion, but chelated with citrate or malate.<sup>21</sup> It has been suggested that these ligands might affect nickel availability for the system, either by impairing transport to the bacteria by chelation or by forming complexes having better interaction with the permease.<sup>29</sup> Consequently we tested the potential effect that the presence of organic acids might have on HupE-mediated nickel transport (Fig. 2). In addition to citrate and malate, we also tested other organic acids likely present in the plant cytoplasm (fumarate, isocitrate, succinate). From these experiments we conclude that the presence of organic acids malate, fumarate and succinate at a concentration of 500  $\mu\text{M}$

did not have a significant effect on Ni uptake through HupE. These data indicate that *R. leguminosarum* HupE is able to extract the ion from the corresponding Ni-organic acid complexes and, also, that these ligands are not required for uptake of this element. In the case of isocitrate and citrate we observed a slight decrease in Ni transport (15–20%) that is consistent with the higher affinity of citrate and isocitrate for nickel.<sup>30</sup> We also tested the effect of the same compounds on Ni uptake mediated by the *E. coli* ATP-dependent NikABCDE transport system. In this case, the presence of citrate and isocitrate resulted in a stronger reduction in the Ni uptake (50% and 25%, respectively) whereas the other organic acids led to a pattern of results similar to those for HupE.

It has been shown that *E. coli* NikABCDE internalizes Ni(II) complexed with L-histidine.<sup>18</sup> To extend the comparative analysis of HupE and NikABCDE systems, we also tested the effect that the presence of L-His might have on Ni transport through HupE. As expected, the presence of high concentrations (500  $\mu\text{M}$ ) of this amino acid resulted in a significant increase in Ni uptake through the Nik system (Fig. 2A). In contrast, the presence of the same L-His concentration originated a drastic reduction (80%) of HupE-mediated transport. Lower concentrations of L-His gradually inhibited Ni uptake by HupE (Fig. 2B). These data suggest that the formation of Ni-(L-His) complexes inhibits transport through HupE, as a probable consequence of the inability of the transporter to extract the metal ion from the complex.

## 2. Effect of metabolic inhibitors

In order to establish the potential energy requirements for nickel transport through HupE,  $^{63}\text{Ni}$  transport assays were performed after exposing HupE-expressing *E. coli* cells to different uncouplers and inhibitors known to affect active transport systems (Table 1). *E. coli* cells expressing the NikABCDE ABC-transporter were included in the assays for comparison. In the experiments with HupE, none of the compounds tested reduced Ni uptake significantly. Furthermore, the presence of compounds known to either dissipate proton motive force (CCCP) or inhibit its generation (azide) resulted in a two-fold increase of HupE-mediated Ni uptake, whereas they significantly

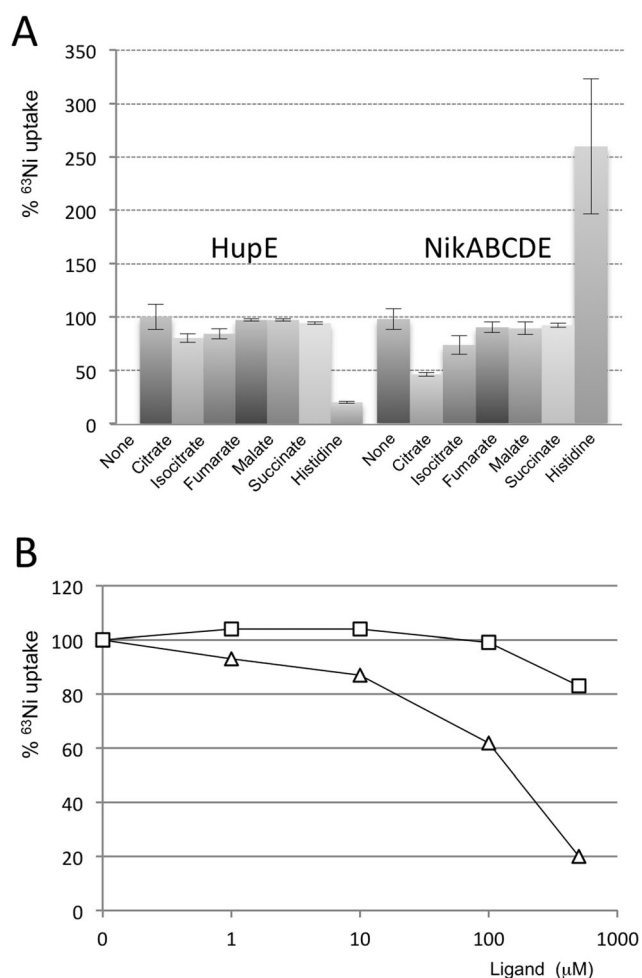


**Fig. 2** Effect of potential Ni ligands on Ni uptake through HupE and Nik transporters. (A) Effect of the presence of the indicated organic acids (500  $\mu\text{M}$ ) and L-histidine (500  $\mu\text{M}$ ) on nickel transport. Assays were performed with *E. coli* HYD723 expressing the indicated transport systems. (B) Effect of increasing concentrations of L-histidine (triangles) and citrate (squares) on Ni uptake by HupE. Values are expressed as percentage of nickel accumulated in the same cells without added compound  $\pm$  S.D. Values on X-axis are on a logarithmic scale. A 100% value corresponds to  $159(\pm 24)$  pmol Ni (mg BDW) $^{-1}$  for HupE1 and to  $10(\pm 2)$  pmol Ni (mg BDW) $^{-1}$  for NikABCDE. S.D. values in (B) were below 5% and are not represented.

**Table 1** Effect of metabolic inhibitors on Ni uptake by *R. leguminosarum* HupE and *E. coli* NikABCDE transporters<sup>a</sup>

Inhibitor	Concentration	Mode of action	% of Ni uptake	
			HupE1	NikABCDE
None			100	100
CCCP	200 $\mu\text{M}$	Protonophore	223 $\pm$ 51	67 $\pm$ 5
Azide	10 mM	Block respiratory chain	196 $\pm$ 11	36 $\pm$ 1
Arsenate	10 mM	Block fermentation	126 $\pm$ 11	79 $\pm$ 5
DCCD	200 $\mu\text{M}$	Block ATPase channel	105 $\pm$ 9	94 $\pm$ 2

<sup>a</sup>  $^{63}\text{Ni}$  transport activities were determined in *E. coli* HYD723 cells with plasmids pBADE1 (HupE1) and pLW22 (NikABCDE) exposed to 150 nM  $^{63}\text{Ni}$  for 5 min. Cells were incubated for 15 min in the presence of inhibitors prior to initiation of the assay. A 100% value corresponds to  $80(\pm 9)$  pmol Ni (mg BDW) $^{-1}$  for HupE1 and to  $11(\pm 2)$  pmol Ni (mg BDW) $^{-1}$  for NikABCDE. Values are relative uptake rates compared to that of samples without added compound.

reduced Ni transport *via* NikABCDE (Table 1). Moreover a control performed with the empty vector pBAD18 did not display the inhibitor-induced phenotype with either CCCP or azide (data not shown), which confirmed that the stimulation was strictly dependent on the functioning of HupE. These results indicate that Ni uptake by HupE is not linked to energy, in contrast to that mediated by NikABCDE which, as expected, occurred by an energy-dependent process. Therefore, transport of Ni by *R. leguminosarum* HupE is consistent with a mechanism of facilitated diffusion. Stimulation of HupE-dependent Ni transport by uncouplers might further suggest the presence of an additional proton motive force-dependent mechanism that could mediate the efflux of Ni from the *E. coli* cells. Alteration of its function by these metabolic inhibitors would lead to an increased accumulation of Ni inside the cells. Alternatively, the destruction of the membrane potential might result in the exit of positive charges of the cell, thus facilitating the import of Ni(II).

Arsenate, an inhibitor of fermentation-derived ATP synthesis, also led to increased HupE-dependent Ni uptake and decreased Ni uptake through the Nik transporter, although the effect was less pronounced than in the case of azide and CCCP. This milder effect could be due to the fact that the assay was not performed under strict anaerobic conditions. This result is also consistent with the notion that ATP hydrolysis is the energy source for NikABCDE activity, and confirmed that HupE-dependent Ni transport is not driven by energy. Finally, addition of the ATP synthase inhibitor DCCD had no effect on either transporter. In the presence of this compound, only the flow of protons through the ATP synthase is blocked, and thus the interconversion of the two cell energy sources, protonmotive force and ATP, is abolished. In the presence of this inhibitor a normal Ni uptake level through NikABCDE was observed, as expected from this ABC-transporter. DCCD did not stimulate HupE-mediated Ni transport, in contrast to the enhancing effect of uncoupler CCCP or respiration inhibitor azide reported above. This agrees with the suggestion of the charge compensating efflux system evoked above, considering that this system is hypothesized to be dependent on the proton motive force that remains unaffected in the presence of DCCD. These data also support the suggestion that the HupE permease operates *via* a mechanism of facilitated diffusion.

### 3. Topological analysis of HupE

A previous topological model for HupE in the cytoplasmic membrane was derived from algorithm-based predictions, which favoured six transmembrane (TM) domains with a periplasmic N-terminal domain. To validate this model, in-frame fusions of parts of the *hupE* gene to  $\beta$ -galactosidase (*lacZ*) and to alkaline phosphatase (*phoA*) reporter genes were constructed, and enzymatic activities were determined in *E. coli* cultures expressing the chimeric proteins (Fig. 3).

High levels of alkaline phosphatase (AP) and low levels of  $\beta$ -galactosidase ( $\beta$ -gal) activities were associated with fusions to residue N35, which is consistent with the predicted location of the N-terminal part of the protein in the periplasm. Also, reporter fusions at residues T56 and I110 showed low AP and

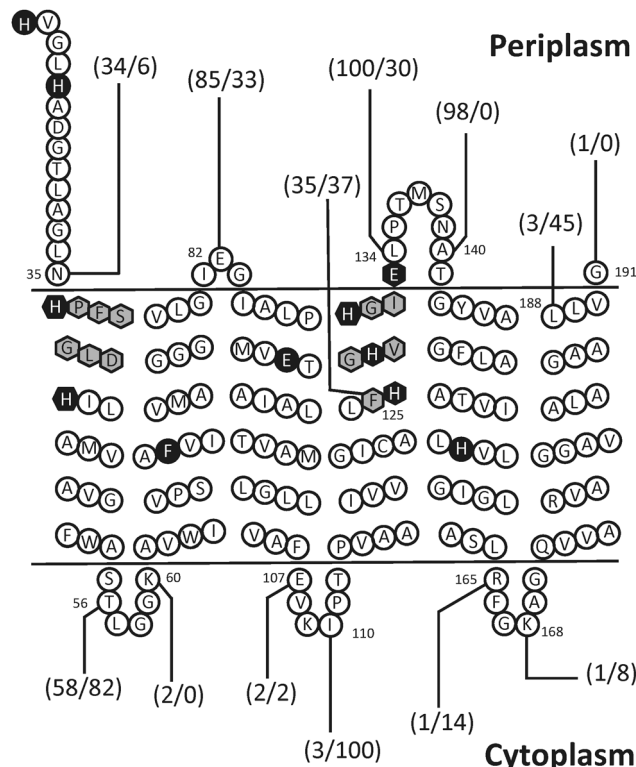


Fig. 3 Topological analysis of *R. leguminosarum* HupE. The values in parentheses linked to specific residues indicate the relative alkaline phosphatase/ $\beta$ -galactosidase activities associated with C-terminal translational fusions to the corresponding reporter genes at these residues. Values are the average of at least two independent determinations. A value of 100% corresponds to 180( $\pm$ 3) units of alkaline phosphatase (fusion to L134), and to 2805( $\pm$ 65) units of  $\beta$ -galactosidase (fusion to I110). Residues shown in black background are those subjected to site-directed mutagenesis, and those in hexagons correspond to the two conserved motifs described previously.<sup>16</sup>

high  $\beta$ -gal levels, which confirms the existence of cytoplasmic loops around these positions. Finally, the high AP and low  $\beta$ -gal levels observed for fusions to residues E82 and L134/A140 denote that these participate in periplasmic loops. The results obtained with the fusions mentioned above confirm the topological model previously proposed for TM domains I–IV,<sup>16</sup> likely the most important ones for protein functionality since they contain the conserved motifs shown to be essential for transport activity (see below). It has to be noted, however, that two of the fusions in this part of the protein (fusions to residues K60 and E107) showed anomalously low values for both activities, suggesting that they originate either unstable proteins or proteins that do not integrate into the membrane. Reporter activities associated with fusions in residues towards the C-terminus of the protein (R165, K168, L188, and G191) did not give a clear pattern of results, since the levels of activity for both reporters were low. These results do not allow a clear assignment of the predicted TM domains V and VI, and suggest that the region corresponding to these two TM segments is buried within the lipid layer.

Overall, the data obtained for the topological analysis confirm the periplasmic location of the N-terminal end of the



protein and the existence of at least five of the TM domains (I through V) predicted in our previous model, and suggest the existence of a *ca.* 50-aa C-terminal domain likely buried in the lipid bilayer.

#### 4. Effect of the alteration of selected HupE residues on Ni uptake

Previous site-directed mutagenesis experiments had shown that several of the HupE histidine residues (H36, H43, and H130) were critical for the ability of the protein to promote hydrogenase activity in a Ni transport-deficient *E. coli* background,<sup>16</sup> whereas the alteration of yet another histidine residue (H126) led to an intermediate phenotype. We have now determined the effect of these mutations on Ni uptake. Additional point mutations affecting four other residues (D42, F69, E90, and E133) conserved in HupE-like proteins were also generated and included in the analysis.

Assays of <sup>63</sup>Ni transport revealed that mutations in histidine residues H36, H43, and H126, previously shown to be relevant for HupE-dependent hydrogenase activity,<sup>16</sup> were associated with reduced levels of Ni uptake activity (Table 2). Also, all four new mutations studied (D42N, F69A, E90Q, and E133Q) significantly reduced both hydrogenase and Ni uptake activities. As expected, the mutations H128I and H155I, previously reported not to affect the levels of hydrogenase activity supported by HupE, led to similar or higher levels of Ni transport compared to wild-type HupE. Overall, these results indicate Ni uptake phenotypes in good correlation with the hydrogenase activities displayed by each of the corresponding mutants.

We also analysed the effect that mutations on the histidine residues located in the N-terminal periplasmic region (H22 and H26) might have on Ni uptake phenotypes (Table 3). The results obtained were consistent with the values of hydrogenase activities. Since the double mutant H22/H26 displayed a significant decrease in both Ni transport and hydrogenase activities, we hypothesized that the presence of both N-terminal histidines might be especially relevant for the Ni uptake process. To test this hypothesis we

**Table 2** Effect of mutations in selected HupE residues on Ni uptake and hydrogenase activity in *E. coli* HYD723 cells<sup>a</sup>

Plasmid	% Ni uptake	% hydrogenase activity
pBADE1 (w.t.)	100	100
pBADE1.H36I	56–359	4 ± 1
pBADE1.D42N	38 ± 10	30 ± 5
pBADE1.H43I	23 ± 3	15 ± 8
pBADE1.F69A	40 ± 7	49 ± 7
pBADE1.E90Q	46 ± 6	56 ± 8
pBADE1.H126I	73 ± 9	36 ± 11
pBADE1.H128I	372 ± 100	115 ± 30
pBADE1.H130I	55–172	11 ± 6
pBADE1.E133Q	37 ± 9	46 ± 9
pBADE1.H155I	131 ± 24	70 ± 4

<sup>a</sup> Values are expressed as percentages of nickel uptake or hydrogenase activity associated with the wild type pBADE1 plasmid. The absolute values (100%) of these parameters for strain HYD723(pBADE1) were 1700 ± 420 nmol H<sub>2</sub> h<sup>-1</sup> (mg protein)<sup>-1</sup> and 42 ± 14 pmol Ni (mg BDW)<sup>-1</sup>, respectively. Values are the average of at least three independent determinations ± S.D.

**Table 3** Effect of mutations of the N-terminal part of HupE on hydrogenase activity and Ni uptake in *E. coli* cells<sup>a</sup>

Plasmid	% Ni uptake	% hydrogenase activity
pBADE1	100	100
pBADE1.H22I	232 ± 46	144 ± 39
pBADE1.H26I	108 ± 10	82 ± 12
pBADE1.H22I/H26I	37 ± 10	42 ± 14
pBADE1.Δ22–27	1137 ± 139	10 ± 2
pBADE1.Δ22–35	53 ± 4	3 ± 1

<sup>a</sup> Transport assays were performed as described in Table 1. The 100% value corresponds to Ni uptake of wild-type protein (42 ± 14 pmol Ni (mg BDW)<sup>-1</sup>). Values are the average of at least three independent determinations.

constructed deleted forms of the protein lacking this region. Mutant Δ22–27 was devoid of residues H22 through A27, whereas mutant Δ22–35 lacked amino acid residues H22 through N35. Both deletions nearly completely abolished hydrogenase activity, indicating that Ni was not transported to the cytoplasm by these protein variants. A significant reduction of the initial Ni uptake rate was shown by the Δ22–35 deletion whereas, unexpectedly, a very high initial Ni uptake rate was associated with deletion Δ22–27. As this mutant does not provide nickel for hydrogenase synthesis, the metal ion might be retained on the truncated transporter, perhaps bound to the aspartic residue (D28) exposed at the N-terminus of the deleted form of the protein.

In order to exclude the possibility of a potential instability caused by the mutations, the presence of the different mutant proteins was verified by in-gel analysis of <sup>35</sup>S-labelled proteins obtained from *E. coli* cultures expressing each of the protein variants. A protein band of the appropriate size (*ca.* 17 kDa) was present in the extract from the HupE-expressing cells and absent in the negative control strain (Fig. S1, ESI†). Analysis of extracts from strains expressing the different mutant variants revealed the presence of bands of similar sizes in all cases. The intensity of this band, referred to the protein load on each lane, was also comparable to that of the wild-type protein for most of the mutants. However, significant reductions in intensity were observed for mutants H43I and H22I/H26I, suggesting that these mutations might decrease protein stability. The same analysis revealed that both N-terminally truncated proteins were present in the cells at levels lower than those corresponding to the wild type (Fig. S1, ESI†), suggesting a role of the periplasmic N-terminal domain in the stability of the protein.

We used the site-directed mutants to study the possible mechanism underlying the increase of HupE-mediated Ni accumulation in response to the presence of uncouplers. Experiments similar to those included in Table 1 were performed using the HupE mutated variants altered in the different residues. As shown in Table 4, the presence of uncouplers azide or CCCP stimulated Ni uptake only when hydrogenase activity displayed by the corresponding HupE variant was close to wild-type levels. This pattern corresponded to mutants allowing Ni delivery for metalloenzyme synthesis, such as H22I, H26I, and H128I. This result suggests that the entry of Ni is required for the observed stimulatory effect of uncouplers,

**Table 4** Effect of CCCP and azide on Ni uptake by *R. leguminosarum* HupE variants

Mutant	% of Ni transport <sup>a</sup>		% of hydrogenase activity
	CCCP	Azide	
pBADE1	220	197	100
pBADE1-H22	141	201	144
pBADE1-H26	205	160	82
pBADE1-D42	46	ND	30
pBADE1-H43	97	123	15
pBADE1-F69	96	ND	49
pBADE1-E90	185	ND	56
pBADE1-H126	101	116	36
pBADE1-H128	277	261	115
pBADE1-E133	148	ND	46
pBADE1-H155	138	ND	70

<sup>a</sup> Transport assays were performed as described in Table 1. Control of Ni transport without addition of uncouplers corresponds to the 100% value. Percentage of hydrogenase activity was taken from values in Table 2. ND, not determined.

and reinforces the hypothesis of the existence of an efflux system in *E. coli* cells that is inhibited by these compounds, thus increasing the net balance of Ni accumulation in the cell. On the other hand, the particular behaviour of E90 and E133, and also D42, all affected in residues contributing negative charges to the protein, suggests that HupE itself might somehow depend on membrane potential.

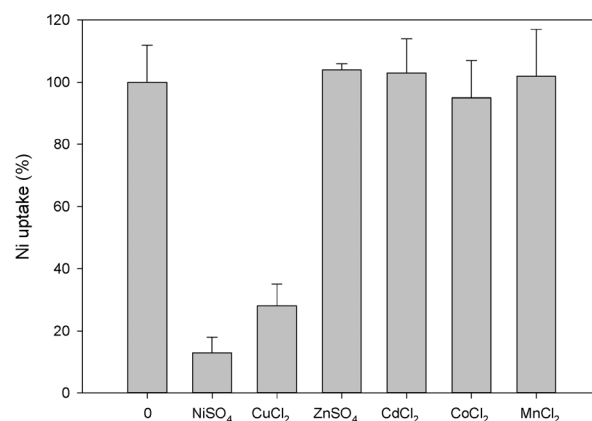
### 5. Specificity of nickel uptake

Evidence derived from sequence analysis indicates that certain members of the HupE/UreJ family transport cobalt instead of nickel.<sup>5</sup> To assess whether HupE could transport other metals in addition to Ni, transport assays were performed in the presence of competing cations. In these experiments we observed that a 50-fold excess of Mn(II), Co(II), Cd(II), or Zn(II) did not significantly affect nickel uptake (Fig. 4A) suggesting that *R. leguminosarum* HupE is highly specific for Ni(II) as regarding these related cations. Surprisingly, addition of 5  $\mu$ M Cu(II) resulted in a clear inhibition of nickel uptake (70% reduction). The degree of inhibition was studied also at lower concentrations of Cu(II), and substantial reduction of <sup>63</sup>Ni uptake was also observed in the presence of just a 10-fold excess of this cation (Fig. 4B). Significantly higher inhibitions were observed when equivalent concentrations of cold Ni(II) were used.

## Discussion

[NiFe] hydrogenases from diazotrophic bacteria play a relevant role in the symbiosis with legume plants, where they recycle molecular hydrogen evolved from nitrogenase, thus improving the energy efficiency of the nitrogen fixation process.<sup>31</sup> We have previously described the involvement of the *R. leguminosarum* Ni permease HupE in the synthesis of hydrogenase under both vegetative and symbiotic conditions.<sup>16</sup> In this work we further provide detailed functional characterization of this nickel transport system following its expression in a *nikABCDE* mutant strain of *E. coli* which is impaired in specific Ni transport.<sup>4</sup>

A



B

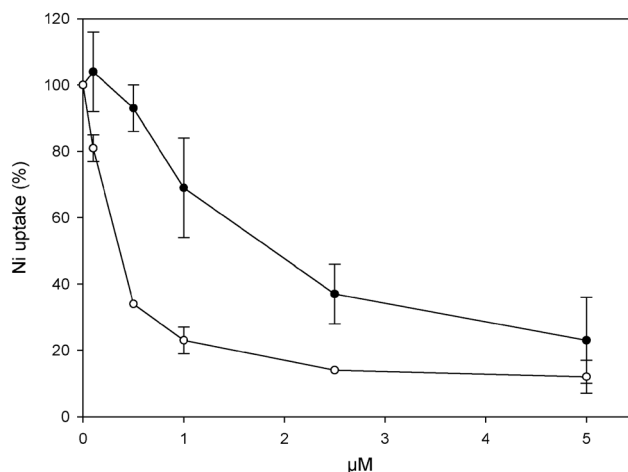


**Fig. 4** Specificity of divalent cation transport through HupE. (A) Bars indicate the relative nickel uptake in *E. coli* cells expressing HupE1 incubated for 5 min with 100 nM <sup>63</sup>Ni alone (0) or in combination with a 50-fold higher concentration of the indicated salts. (B) Kinetics of inhibition of <sup>63</sup>Ni uptake by cold Ni(II) (open circles) or Cu(II) ions (closed circles) added at the indicated concentrations. In all cases the 100% of activity corresponds to that of *E. coli* HYD723(pBADE1) cells incubated in the presence of 100 nM <sup>63</sup>Ni [59(±7) pmol Ni (mg BDW)<sup>-1</sup>].

### Kinetics of nickel transport

The observed values for the apparent  $K_m$  (227 nM) and  $V_{max}$  (49 pmol Ni<sup>2+</sup> transported min<sup>-1</sup> (mg BDW)<sup>-1</sup>) kinetic parameters indicate that the HupE permease is a medium-affinity and low-capacity transporter. Comparison of the  $K_m$  value with those reported previously for the NiCoT permeases HoxN of *C. necator* (20 nM<sup>10</sup>) and NixA of *H. pylori* (11 nM<sup>9</sup>) and more recently for the NikABCDE ABC-transporter of *E. coli* (33 nM<sup>18</sup>) shows that the affinity of HupE for nickel is substantially lower. In contrast, kinetic analyses of Ni uptake measured in strains SR and SR470 of another nitrogen-fixing bacterium, *B. japonicum*, where the HoxN-related permease HupN was subsequently identified,<sup>32</sup> revealed a 100-fold higher apparent  $K_m$  (26–50  $\mu$ M<sup>28</sup>) relative to that of HupE. Intermediate values in the micromolar range were measured in the acetogen *C. thermoacetica*<sup>23</sup> and in the methanogen *M. bryantii*,<sup>24</sup> which require the nickel-dependent

enzyme complex acetyl-CoA synthase/carbon monoxide dehydrogenase for chemolithotrophic growth. The medium-affinity HupE system presumably accounts for the ability of *R. leguminosarum* to grow in symbiosis with legume plants and is consistent with the levels of Ni present in the lentil or pea nodule cytosols surrounding the bacteroids.<sup>21,29</sup>

In general, low rates of accumulation have been associated with nickel transport systems examined so far in a variety of microorganisms independently of the growth conditions.<sup>24,33</sup> This also applies for *R. leguminosarum* HupE, which shows a maximal velocity of 49 pmol Ni<sup>2+</sup> transported min<sup>-1</sup> (mg BDW)<sup>-1</sup>. However, this low rate of uptake is efficient enough to allow appropriate Ni accumulation for the synthesis of high hydrogenase activity in the *E. coli* host (Table 2;<sup>16</sup>) that reached the values measured in bacteroid cells under the natural symbiotic conditions.<sup>16</sup> The low  $V_{\max}$  possibly protects the cells from the toxic effects of nickel<sup>34</sup> and also indicates that these organisms do not require much nickel for growth.

In symbiosis, nickel ions are obtained from the plant cytosol surrounding the bacteroids, and it has been shown that nickel is not present as a free ion but rather as complexes with the organic ligands citrate or malate.<sup>21</sup> Our results show that the nature of the nickel forms does not influence the rate of HupE-dependent Ni uptake, with the exception of added L-His that acts as a strong inhibitor (Fig. 2). This is consistent with our observation that the presence of citrate and malate did not affect the induction of hydrogenase activity in *R. leguminosarum* cultured cells (our unpublished results). Efficiency of the NikABCDE-dependent Ni transport in *E. coli* cells increases when Ni is complexed with (L-His)<sub>2</sub>.<sup>18</sup> Consistently, the crystal structure of the periplasmic nickel-binding protein NikA of *E. coli* in complex with Ni-(L-His)<sub>2</sub> has been subsequently described.<sup>35</sup> More recently, a similar crystal structure of the analogous CeuE periplasmic component that is supposed to be involved in nickel/cobalt acquisition together with the ABC-transporter components FecD/FecE in *H. pylori* has also been reported.<sup>19</sup> However, the real physiological nature of the ligand awaits further investigation. Indeed, a previous structure of the native periplasmic protein NikA obtained after purification from the growth media without any additive is in favour of the existence of a tricarboxylated molecule as the natural nickelophore.<sup>17</sup> Our data show that the mechanism of Ni import in *R. leguminosarum* is clearly distinct from that in *E. coli*, and also exclude the role of the two major organic chelators present in legume nodules, citrate and malate, facilitating Ni transport in *R. leguminosarum*. However, we cannot rule out the possibility that *R. leguminosarum* synthesizes another nickelophore or uses another Ni ligand complex to internalize Ni. A potential TonB-dependent nickel transporter across the outer membrane has been identified by genomic analysis in *B. japonicum*.<sup>36</sup> However, no such transporter has been identified in *R. leguminosarum* so far.

### Energetics of transport

Here we show unambiguously that Ni transport by *R. leguminosarum* is not driven by a primary or secondary active transport mechanism, in contrast to that mediated by *E. coli* NikABCDE which relies on ATP

hydrolysis (Table 1). This finding is in favor of the fact that the HupE permease functions *via* a mechanism of facilitated diffusion. There are a few cases in which Ni transport has been suggested to occur by an energy-independent mechanism as in *Azotobacter chroococcum*<sup>37</sup> and in *B. japonicum*.<sup>28</sup> The existence of an energy-independent Ni uptake system implies that nickel ions will move across the cytoplasmic membrane down their concentration gradient. Therefore, accumulation of Ni inside the cells would result from an efficient cellular metabolism which allows a rapid incorporation of the metal into the nickel-dependent hydrogenases through the participation of a variety of accessory proteins (for a review, see ref. 38). Also, the propensity of Ni to tightly bind to various biomolecules<sup>39</sup> may contribute to the outside-inside Ni gradient and thus facilitate its transport. In this study, compounds that block ATP synthesis by either dissipating the proton motive force (CCCP, azide) or inhibiting the fermentation (arsenate) significantly stimulated Ni transport by HupE while reducing Ni uptake by NikABCDE. This observation suggests that Ni import by HupE is coupled to a proton motive force-dependent efflux system able to export Ni ions, whose activity is abolished in the presence of uncouplers, leading to an increase in the level of intracellular <sup>63</sup>Ni radioactivity. A possible candidate might be the RcnAB pump of *E. coli*<sup>40,41</sup> that has been demonstrated to export Ni and Co ions, helping the bacteria to overcome the toxicity of both metals when they are in excess. We do not know whether the basal level of RcnAB present in the conditions of our uptake assay would be sufficient to get rid of Ni, but measurement of HupE-mediated Ni transport in an *rcnA-nikA* background could help to clarify this. In the original *R. leguminosarum* background a Ni- and Co-efflux system (DmeRF) is known to operate, and its role has been connected to the uptake of nickel.<sup>42</sup>

Alternatively, another electrogenic efflux system could act as a charge-compensating mechanism by extruding positive charges out of the cell. Our uptake mixture is made of a potassium phosphate (KH<sub>2</sub>/K<sub>2</sub>HPO<sub>4</sub>) buffer containing 10 mM MgCl<sub>2</sub>. CorA, the nonspecific constitutively expressed major Mg<sup>2+</sup> transporter, can mediate Mg efflux at relatively high extracellular Mg concentrations (1 mM) and this efflux is maximal at 10 mM extracellular Mg,<sup>43</sup> which corresponds to the concentration that we used in our transport assay. Therefore it is tempting to speculate that Mg efflux *via* CorA could compensate positive charges during Ni uptake. Moreover, *E. coli* possesses a multiplicity of K<sup>+</sup> energy-coupled efflux systems that could also participate in the process.<sup>44</sup>

### Topological analysis

HupE is shown here to have a periplasmic N-terminal domain. This is different from the topological model of the two NiCoT transporters NixA and HoxN whose amino termini are located in the cytoplasm.<sup>12,27</sup> This difference might be related to the fact that NiCoT proteins do not have a signal peptide, whereas a canonical 21-amino acid signal peptide is present in HupE.<sup>16</sup> Deletion of the N-terminal part of HupE nearly suppressed hydrogenase activity (Table 3) and also severely impaired the stability of the expressed mutated variants (Fig. S1, ESI<sup>†</sup>),

enlightening the fact that the presence of the amino terminus was crucial to ensure the normal function of the transporter. The apparent Ni uptake displayed by these mutants was merely due to its retention in the periplasm or its binding at the outer surface of the cytoplasmic membrane. Reporter gene fusion activities have confirmed most of the topological determinants previously predicted by bioinformatic analyses, including the presence of two cytoplasmic and two periplasmic loops defining at least five transmembrane domains (Fig. 3), in contrast to the NiCoT proteins which possess eight transmembrane domains. Results regarding the C-terminal domain of HupE, including the previously predicted transmembrane domains V and VI, are less clear since reporter activities are much lower. A possible explanation is that this part of the protein is buried in the lipid bilayer. Alternatively, fusion proteins in this part of HupE could be more unstable. Mutation of the only histidine residue located in this region, H155, had no significant effect on the rate of nickel import (Table 2), suggesting that this domain might not participate in the direct translocation of Ni ions.

### Identification of essential residues

According to the topological data, the two conserved motifs in the HupE/UreJ family, HX<sub>5</sub>DH and FHGX[AV]HGXE, are located in the transmembrane domains I and IV, respectively. Site-directed mutations of conserved histidines in these motifs, H36I, H43I, H126I and H130I, which have been shown to severely reduce hydrogenase activity<sup>16</sup> affected the initial rate of Ni uptake to various degrees. Additional mutations in other conserved residues (F69A, E90Q and E133Q located in helices II, III and IV, respectively) diminished Ni transport and hydrogenase activity in a correlated manner. Overall, these data suggest that these four transmembrane domains are directly involved in binding and translocation of Ni ions, likely constituting a pore through which Ni could pass. The first motif, HX<sub>5</sub>DH, is highly similar to that described in the NiCoT permease family as essential for Ni uptake,<sup>11</sup> whereas the second motif, FHGX[AV]HGXE, is very different and may define a novel way for Ni ions to cross the membrane. It is not known how these motifs participate in the forming of a pore, and we have no information about the number of HupE monomers that could be involved in such a pore. Small transport proteins with six membrane-spanning domains are likely to function as multimers, mainly dimers.<sup>45</sup>

### Specificity for nickel

Competition analysis with several other metal ions showed that HupE discriminates nickel *versus* cobalt ions, even when cobalt was present at 50-fold concentrations. This high selectivity for nickel *versus* cobalt ions is also a characteristic of Class I NiCoT transporters such as HoxN.<sup>46</sup> The basis for this selectivity has been traced to determinants located in transmembrane domains I and II from HoxN.<sup>47</sup>

The interference of Cu<sup>2+</sup> with HupE-mediated Ni uptake is intriguing. However, similar levels of inhibition have been reported for the Ni transport in *B. japonicum*<sup>28</sup> and in *R. rubrum*.<sup>48</sup> Other metal transporters, such as the *E. coli* zinc transporter ZupT,

are supposed to transport also copper, thus inducing higher sensitivity to this metal.<sup>49</sup> In contrast, HupE-expressing *R. leguminosarum* and *E. coli* cells were not more sensitive to copper (data not shown). Attempts were made to assess whether the inhibition by copper ions was competitive or not competitive through the determination of  $K_m$  and  $V_{max}$  parameters in the presence of different amounts of Cu(II). Unfortunately, no conclusive results were obtained in this analysis (data not shown). The observed blocking effect could be due to the high affinity of copper for different molecules as deduced from its top position at the Irving-Williams series. Copper ions are also able to bind NikR, and a similar planar geometry for the binding of both Cu and Ni ions has been described.<sup>50</sup> It is tempting to speculate that Cu is blocking the access to Ni ions by binding at some specific positions of the HupE protein, but more detailed experimentation is required to elucidate this point.

## Materials and methods

### Bacterial strains, plasmids, and growth conditions

*E. coli* strains were routinely grown at 37 °C in LB medium.<sup>51</sup> For induction of hydrogenase activity in *E. coli* cells, strain HYD723<sup>52</sup> was grown at 28 °C under anaerobic conditions in a modified TGYEP medium<sup>53</sup> containing glycerol (0.4%) and fumarate (20 mM). Antibiotic concentrations used were as follows (μg ml<sup>-1</sup>): ampicillin, 100 and kanamycin, 50.

### DNA manipulation techniques

DNA manipulations including purification, restriction, ligation, agarose gel electrophoresis, PCR amplification, and transformation into *E. coli* cells were carried out by standard methods.<sup>54</sup> *E. coli* DH5α was used for standard cloning procedures.<sup>55</sup>

### Mutant and plasmid constructions

Site-directed mutagenesis of the *hupE* gene was carried out as previously described.<sup>16</sup> The primers used for mutant constructions D42N, F69A, E90Q and E133Q are included in Table S1 (ESI†). Truncated forms of HupE with in-frame deletions removing either partially (residues H22 through A27) or fully (residues H22 through N35) the N-terminal region of the protein were synthesized by a commercial company (GenScript, USA) and cloned in vector pUC57 (Genscript, USA). In these constructs the sequence coding for the ribosome binding site 5'-AGGAGGAATTCACC-3' was fused at the 5' of the *hupE* coding sequence. The entire sequence was excised with *NheI* and *SalI* and cloned in vector pBAD18-Kan.<sup>56</sup> In order to study the stability and expression of the mutated versions of HupE, DNA containing the protein variants was excised with *NheI* and *HindIII* and cloned (*XbaI/HindIII*) downstream the T7 RNA polymerase-promoter from vector PCR2.1-TOPO.

For topology studies of HupE, translational fusions between different lengths of the N-terminal part of HupE and the reporter enzymes alkaline phosphatase (PhoA) and β-galactosidase (LacZ) were generated. Residues corresponding to cytoplasmic, periplasmic, and transmembrane domains predicted in the topological model previously described<sup>16</sup> were chosen as fusion sites. DNA fragments of



the *hupE* gene encoding N-terminal regions of the protein up to amino acids N35, T56, K60, E82, E107, I110, F125, L134, A140, R165, K168, L188 and G191 were amplified by PCR using plasmid pBADE1<sup>16</sup> as a template and a primer incorporating a *KpnI* site in forward primer EChupE1-Kpn (common to all fragments), and a *XbaI* site in reverse primers pN35-X through pG191-X (Table S1, ESI†). The amplified DNA fragments were cloned in plasmid PCR2.1-TOPO, excised with *KpnI* and *XbaI* and cloned in the reporter fusion vectors pECD636 and pECD637, pGEM-T-Easy derivatives of pECD499 and pECD500, respectively.<sup>57</sup> The sequence of the PCR products and the correct reading frame at the fusion sites were confirmed by sequencing.

### Determination of alkaline phosphatase and $\beta$ -galactosidase activities

To measure the enzymatic activities the procedure of Solis-Oviedo *et al.*<sup>58</sup> was used as described. Bacterial cultures of *E. coli* strain CC118(pGP1-2)<sup>59,60</sup> harboring the *lacZ* or *phoA* fusions were grown in LB medium at 30 °C to an optical density (OD<sub>600</sub>) of ca. 0.4. Then, cultures were incubated at 42 °C for 30 minutes to induce the expression of the T7 RNA polymerase, and reporter activities were monitored by measuring alkaline phosphatase<sup>61</sup> or  $\beta$ -galactosidase<sup>51</sup> activities using *p*-nitrophenyl-phosphate (*p*NPP) or *o*-nitrophenyl-galactopyranoside (ONPG), respectively, as substrates. Enzyme activities were calculated as the change of absorbance at 420 nm per minute per unit of absorbance at 600 nm (cell turbidity). Values were normalized using the highest value measured as 100%.

### Hydrogenase activity assays

Hydrogenase activity was induced in bacterial cultures of *E. coli* HYD723 grown under anaerobic conditions as previously described.<sup>16</sup> Hydrogenase activity was measured by an amperometric method using a Clark-type hydrogen sensor (Unisense©, Denmark) with oxygen as electron acceptor.<sup>62</sup> Protein content of cell suspensions was determined by the bicinchoninic acid method<sup>63</sup> after alkaline digestion of cells at 90 °C in NaOH for 10 min, with bovine serum albumin as the standard.

### Nickel transport assays

*E. coli* strain HYD723 carrying plasmid pBADE1 or derivative plasmids expressing the *R. leguminosarum* HupE permease was grown under aerobic conditions in LB medium, whereas *E. coli* strain HYD723 carrying plasmid pLW22<sup>64</sup> expressing the *E. coli* NikABCDE ABC-transporter was cultivated anaerobically in LB medium supplemented with molybdate and selenite, as previously described.<sup>4</sup> Nickel transport assays were performed essentially as described.<sup>16</sup> Cells were suspended in the reaction mixture (65 mM KH<sub>2</sub>PO<sub>4</sub>–K<sub>2</sub>HPO<sub>4</sub> [pH 6.8], 11 mM glucose, 10 mM MgCl<sub>2</sub>) to a final concentration of 0.3–0.4 mg BDW ml<sup>–1</sup> for HYD723(pBADE1) and 2–3 mg BDW ml<sup>–1</sup> for HYD723(pLW22). The assay was initiated by the addition of <sup>63</sup>NiCl<sub>2</sub> (3.78 mCi ml<sup>–1</sup>; 0.225 mg Ni ml<sup>–1</sup>; Brookhaven National Laboratory). Samples (200  $\mu$ L) were taken at regular time intervals, vacuum filtered through 0.45  $\mu$ m cellulose nitrate membrane filters (Millipore), and washed twice with 10 mM EDTA in phosphate buffer. After drying, the filters were transferred to scintillation vials with 5 mL

scintillation fluid (Ultima Gold F, Perkin Elmer) for counting in a Packard Tricarb 2100 scintillation counter. Control values obtained from HYD723 carrying the empty vector pBAD18 were subtracted to correct for non-specific <sup>63</sup>Ni binding.

For kinetic parameter determination, the uptake assay was performed with the addition of 50 to 1000 nM <sup>63</sup>Ni. Initial linear uptake rates were used to calculate the *K<sub>m</sub>* and *V<sub>max</sub>* parameters using a nonlinear regression curve (Sigma Plot 12.5 software).

The effect of organic acids and L-Histidine on Ni uptake was measured in the presence of 150 nM <sup>63</sup>Ni over a 5 min incubation period. Potential ligands were added 1 min prior to addition of radioactive nickel. A similar assay was performed with metabolic inhibitors. Cells were incubated with each inhibitor for 15 min prior to starting the assay.

The cation specificity was examined by using a 50-fold excess (5  $\mu$ M) of each metal (CdCl<sub>2</sub>, CoCl<sub>2</sub>, CuCl<sub>2</sub>, MnCl<sub>2</sub>, NiSO<sub>4</sub>, or ZnSO<sub>4</sub>) relative to <sup>63</sup>Ni (100 nM).

### Expression and labelling of HupE proteins in *E. coli*

Wild-type and mutated versions of HupE were expressed in *E. coli* cells by using the bacteriophage T7 RNA polymerase-promoter system from PCR1.2-TOPO as described by Tabor and Richardson.<sup>60</sup> *E. coli* strain BL21(DE3) was used as an expression host. Cells were labelled with [<sup>35</sup>S] methionine–[<sup>35</sup>S] cysteine mix (Perkin Elmer) as described by Studier and Moffat,<sup>65</sup> and crude extracts were analyzed by sodium dodecyl sulfate-polyacrylamide gel electrophoresis (SDS-PAGE).

## Conclusion

Characterization of *R. leguminosarum* HupE has provided a refined topological and functional model for this nickel permease. HupE is a medium-affinity, nickel-specific permease showing an energy-independent mechanism for moving nickel across the membrane. These results highlight the existence of cell systems that maintain low intracellular nickel levels allowing a positive out-in gradient driving nickel import, and suggest the requirements of balancing processes to maintain metal homeostasis in the cell.

## Acknowledgements

We thank J. Cayron for technical assistance with gel analysis of HupE mutants, and Anabel Bautista for reporter enzyme activity determination. This work was supported by grants from Spain's Ministry of Science and Innovation (BIO2010-15301 and BIO2013-43040 to J.P.), from Fundación Ramón Areces (to J.I.) and by a PICS grant (SYMBIONI no 5992) from the Centre National de la Recherche Scientifique (to A.R.).

## References

- 1 J. L. Boer, S. B. Mulrooney and R. P. Hausinger, *Arch. Biochem. Biophys.*, 2014, **544**, 142–152.

- 2 S. B. Mulrooney and R. P. Hausinger, *FEMS Microbiol. Rev.*, 2003, **27**, 239–261.
- 3 A. M. Sydor and D. B. Zamble, *Met. Ions Life Sci.*, 2013, **12**, 375–416.
- 4 C. Navarro, L. F. Wu and M. A. Mandrand-Berthelot, *Mol. Microbiol.*, 1993, **9**, 1181–1191.
- 5 D. A. Rodionov, P. Hebbeln, M. S. Gelfand and T. Eitinger, *J. Bacteriol.*, 2006, **188**, 317–327.
- 6 K. de Pina, C. Navarro, L. McWalter, D. H. Boxer, N. C. Price, S. M. Kelly, M. A. Mandrand-Berthelot and L. F. Wu, *Eur. J. Biochem.*, 1995, **227**, 857–865.
- 7 P. Hebbeln and T. Eitinger, *FEMS Microbiol. Lett.*, 2004, **230**, 129–135.
- 8 L. Wolfram, B. Friedrich and T. Eitinger, *J. Bacteriol.*, 1995, **177**, 1840–1843.
- 9 H. L. Mobley, R. M. Garner and P. Bauerfeind, *Mol. Microbiol.*, 1995, **16**, 97–109.
- 10 G. Eberz, T. Eitinger and B. Friedrich, *J. Bacteriol.*, 1989, **171**, 1340–1345.
- 11 T. Eitinger, L. Wolfram, O. Degen and C. Anthon, *J. Biol. Chem.*, 1997, **272**, 17139–17144.
- 12 J. F. Fulkerson, Jr. and H. L. Mobley, *J. Bacteriol.*, 2000, **182**, 1722–1730.
- 13 J. F. Fulkerson, Jr., R. M. Garner and H. L. Mobley, *J. Biol. Chem.*, 1998, **273**, 235–241.
- 14 T. Eitinger, J. Suhr, L. Moore and J. A. Smith, *BioMetals*, 2005, **18**, 399–405.
- 15 D. A. Rodionov, A. G. Vitreschak, A. A. Mironov and M. S. Gelfand, *J. Biol. Chem.*, 2003, **278**, 41148–41159.
- 16 B. Brito, R. I. Prieto, E. Cabrera, M. A. Mandrand-Berthelot, J. Imperial, T. Ruiz-Argüeso and J. M. Palacios, *J. Bacteriol.*, 2010, **192**, 925–935.
- 17 M. V. Cherrier, C. Cavazza, C. Bochot, D. Lemaire and J. C. Fontecilla-Camps, *Biochemistry*, 2008, **47**, 9937–9943.
- 18 P. T. Chivers, E. L. Benanti, V. Heil-Chapdelaine, J. S. Iwig and J. L. Rowe, *Metallomics*, 2012, **4**, 1043–1050.
- 19 M. M. Shaik, L. Cendron, M. Salamina, M. Ruzzene and G. Zanotti, *Mol. Microbiol.*, 2014, **91**, 724–735.
- 20 K. Schauer, B. Gouget, M. Carriere, A. Labigne and H. de Reuse, *Mol. Microbiol.*, 2007, **63**, 1054–1068.
- 21 C. Cacho, B. Brito, J. Palacios, C. Perez-Conde and C. Camara, *Talanta*, 2010, **83**, 78–83.
- 22 P. M. Jones and A. M. George, *Crit. Rev. Biochem. Mol. Biol.*, 2013, **48**, 39–50.
- 23 L. L. Lundie, Jr., H. C. Yang, J. K. Heinonen, S. I. Dean and H. L. Drake, *J. Bacteriol.*, 1988, **170**, 5705–5708.
- 24 K. F. Jarrell and G. D. Sprott, *J. Bacteriol.*, 1982, **151**, 1195–1203.
- 25 P. M. Campbell and G. D. Smith, *Arch. Biochem. Biophys.*, 1986, **244**, 470–477.
- 26 M. Lohmeyer and C. Friedrich, *Arch. Microbiol.*, 1987, **149**, 130–135.
- 27 T. Eitinger and B. Friedrich, in *Transition metals in microbial metabolism*, ed. G. Winkelmann and C. J. Carrano, Harwood, Amsterdam, 1997, pp. 235–256.
- 28 L. W. Stults, S. Mallick and R. J. Maier, *J. Bacteriol.*, 1987, **169**, 1398–1402.
- 29 B. Brito, A. Toffanin, R. I. Prieto, J. Imperial, T. Ruiz-Argüeso and J. M. Palacios, *Mol. Plant-Microbe Interact.*, 2008, **21**, 597–604.
- 30 T. Furia, in *CRC Handbook of food additives*, ed. T. Furia, CRC Press, Boca Raton, Florida, USA, 1972, vol. 1, pp. 271–294.
- 31 C. Baginsky, B. Brito, J. Imperial, T. Ruiz-Argüeso and J. M. Palacios, *Appl. Environ. Microbiol.*, 2005, **71**, 7536–7538.
- 32 C. Fu, S. Javedan, F. Moshiri and R. J. Maier, *Proc. Natl. Acad. Sci. U. S. A.*, 1994, **91**, 5099–5103.
- 33 T. Eitinger and M. A. Mandrand-Berthelot, *Arch. Microbiol.*, 2000, **173**, 1–9.
- 34 L. Macomber and R. P. Hausinger, *Metallomics*, 2011, **3**, 1153–1162.
- 35 H. Lebrette, M. Iannello, J. C. Fontecilla-Camps and C. Cavazza, *J. Inorg. Biochem.*, 2013, **121**, 16–18.
- 36 K. Schauer, D. A. Rodionov and H. de Reuse, *Trends Biochem. Sci.*, 2008, **33**, 330–338.
- 37 C. D. Partridge and M. G. Yates, *Biochem. J.*, 1982, **204**, 339–344.
- 38 Y. Li and D. B. Zamble, *Chem. Rev.*, 2009, **109**, 4617–4643.
- 39 K. S. Kasprzak and K. Salnikow, in *Met. Ions Life Sci.*, ed. A. Sigel, H. G. Sigel and R. K. O. Sigel, Wiley, Chichester, 2007, pp. 619–660.
- 40 C. Bleriot, G. Effantin, F. Lagarde, M. A. Mandrand-Berthelot and A. Rodrigue, *J. Bacteriol.*, 2011, **193**, 3785–3793.
- 41 A. Rodrigue, G. Effantin and M. A. Mandrand-Berthelot, *J. Bacteriol.*, 2005, **187**, 2912–2916.
- 42 L. Rubio-Sanz, R. I. Prieto, J. Imperial, J. M. Palacios and B. Brito, *Appl. Environ. Microbiol.*, 2013, **79**, 6414–6422.
- 43 D. G. Kehres and M. E. Maguire, *BioMetals*, 2002, **15**, 261–270.
- 44 M. V. Radchenko, K. Tanaka, R. Waditee, S. Oshimi, Y. Matsuzaki, M. Fukuhara, H. Kobayashi, T. Takabe and T. Nakamura, *J. Biol. Chem.*, 2006, **281**, 19822–19829.
- 45 C. F. Higgins, *Nature*, 2007, **446**, 749–757.
- 46 O. Degen, M. Kobayashi, S. Shimizu and T. Eitinger, *Arch. Microbiol.*, 1999, **171**, 139–145.
- 47 O. Degen and T. Eitinger, *J. Bacteriol.*, 2002, **184**, 3569–3577.
- 48 R. K. Watt and P. W. Ludden, *J. Bacteriol.*, 1999, **181**, 4554–4560.
- 49 G. Grass, M. D. Wong, B. P. Rosen, R. L. Smith and C. Rensing, *J. Bacteriol.*, 2002, **184**, 864–866.
- 50 S. Leitch, M. J. Bradley, J. L. Rowe, P. T. Chivers and M. J. Maroney, *J. Am. Chem. Soc.*, 2007, **129**, 5085–5095.
- 51 J. H. Miller, *Experiments in molecular genetics*, Cold Spring Harbour Laboratory Press, New York, 1972.
- 52 L. F. Wu, M. A. Mandrand-Berthelot, R. Waugh, C. J. Edmonds, S. E. Holt and D. H. Boxer, *Mol. Microbiol.*, 1989, **3**, 1709–1718.
- 53 R. Rossmann, G. Sawers and A. Böck, *Mol. Microbiol.*, 1991, **5**, 2807–2814.
- 54 J. Sambrook and D. W. Russell, *Molecular cloning: a laboratory manual*, Cold Spring Harbor, NY, 3rd edn, 2001.
- 55 D. Hanahan, *J. Mol. Biol.*, 1983, **166**, 557–580.
- 56 L. M. Guzmán, D. Belin, M. J. Carson and J. Beckwith, *J. Bacteriol.*, 1995, **177**, 4121–4130.

- 57 C. Rensing, T. Pribyl and D. H. Nies, *J. Bacteriol.*, 1997, **179**, 6871–6879.
- 58 R. L. Solis-Oviedo, F. Martinez-Morales, O. Geiger and C. Sohlenkamp, *Biochim. Biophys. Acta*, 2012, **1821**, 573–581.
- 59 C. Manoil and J. Beckwith, *Proc. Natl. Acad. Sci. U. S. A.*, 1985, **82**, 8129–8133.
- 60 S. Tabor and C. C. Richardson, *Proc. Natl. Acad. Sci. U. S. A.*, 1985, **82**, 1074–1078.
- 61 E. Brickman and J. Beckwith, *J. Mol. Biol.*, 1975, **96**, 307–316.
- 62 T. Ruiz-Argüeso, F. J. Hanus and H. J. Evans, *Arch. Microbiol.*, 1978, **116**, 113–118.
- 63 P. K. Smith, R. I. Krohn, G. T. Hermanson, A. K. Mallia, F. H. Gartner, M. D. Provenzano, E. K. Fujimoto, N. M. Goeke, B. J. Olson and D. C. Klenk, *Anal. Biochem.*, 1985, **150**, 76–85.
- 64 L. F. Wu, C. Navarro and M. A. Mandrand-Berthelot, *Gene*, 1991, **107**, 37–42.
- 65 F. W. Studier and B. A. Moffatt, *J. Mol. Biol.*, 1986, **189**, 113–130.